YMTHE, Volume *28*

Supplemental Information

Rescue of Advanced Pompe Disease in Mice with Hepatic Expression of Secretable Acid α-Glucosidase

Umut Cagin, Francesco Puzzo, Manuel Jose Gomez, Maryse Moya-Nilges, Pauline Sellier, Catalina Abad, Laetitia Van Wittenberghe, Nathalie Daniele, Nicolas Guerchet, Bernard Gjata, Fanny Collaud, Severine Charles, Marcelo Simon Sola, Olivier Boyer, Jacomina Krijnse-Locker, Giuseppe Ronzitti, Pasqualina Colella, and Federico Mingozzi

Supplemental figure 1

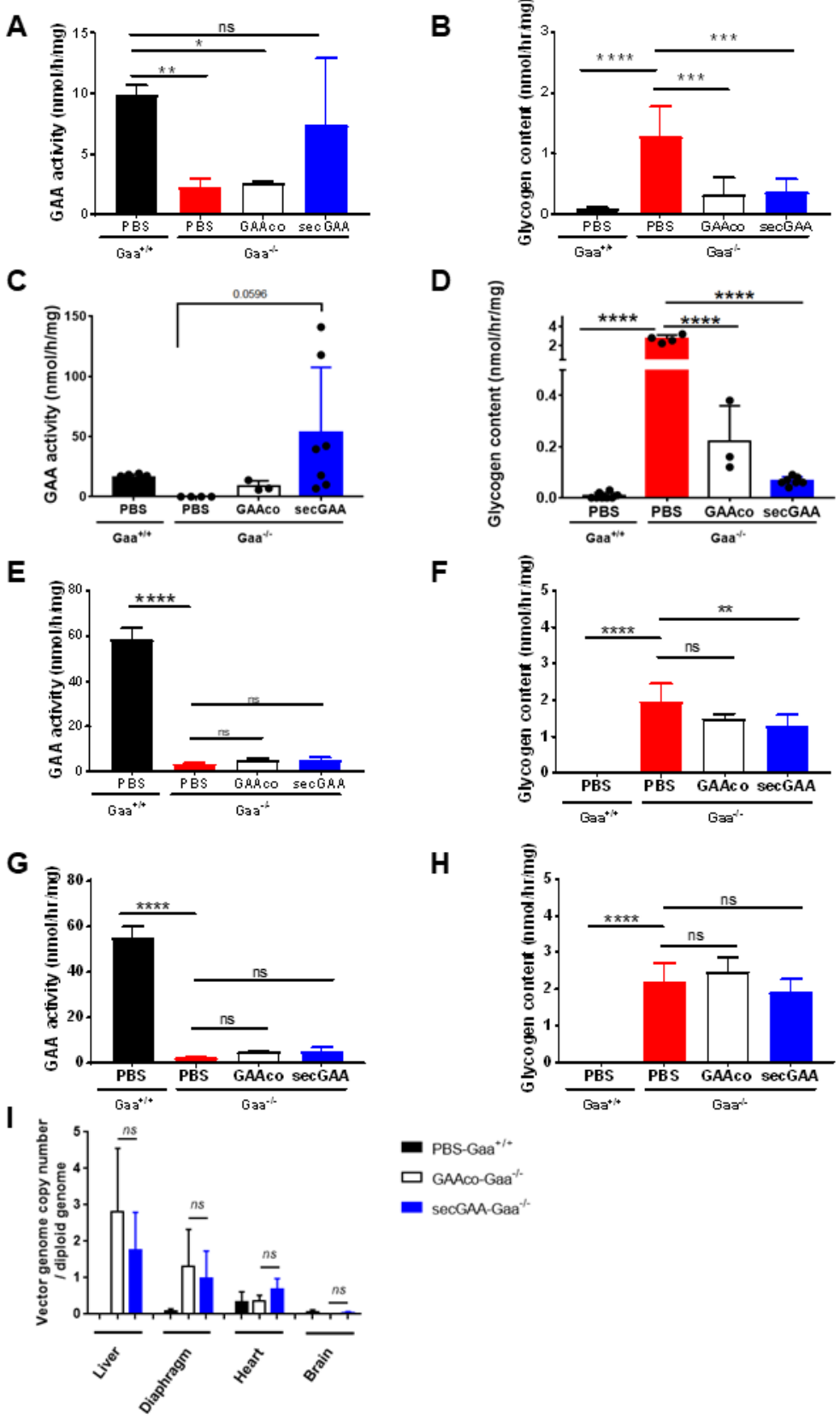

Figure S1. Liver expression of secretable GAA rescues PD at low vector doses. (A-I) Four-month-old $Gaa^{-/-}$ mice were injected with an AAV8-GAAco (GAAco-$Gaa^{-/-}$) or AAV8-secGAA (secGAA-$Gaa^{-/-}$) vector at a dose of $5x10^{11}$ vg/kg. $Gaa^{+/+}$ (PBS-$Gaa^{+/+}$) and $Gaa^{-/-}$ (PBS-$Gaa^{-/-}$) mice injected with PBS served as controls in the study. Animals were followed for ten months after treatment (n=7/8 per cohort). **(A-H)** GAA enzymatic activity and glycogen content in the triceps **(A-B)**, heart **(C-D)**, brain **(E-F)** and spinal cord **(G-H)**. **(I)** Vector genome copy number in the liver ten months post treatment. Statistical analysis: **(A-I)** One-way ANOVA with Tukey's post hoc. ns, not significant; *, $p<0.05$; **, $p<0.01$; ***, $p<0.001$; ****, $p<0.0001$. In graphs C and D each dot represents individual mice. In all graphs error bars represent the standard deviation of the mean.

Supplemental figure 2

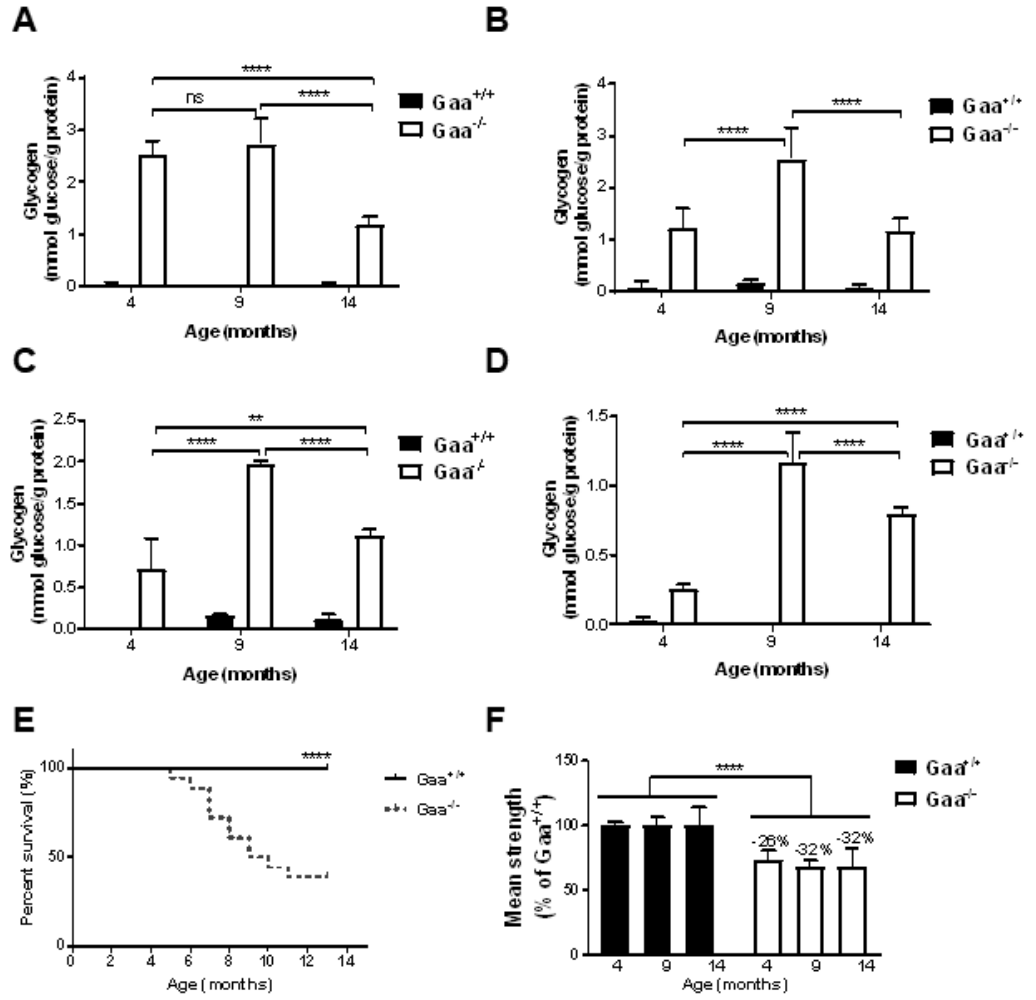

Figure S2. Evolution of the disease phenotype in Gaa$^{-/-}$ mice at different ages. (A-D) Glycogen content in heart **(A)**, diaphragm **(B)**, triceps **(C),** and brain **(D)** of Gaa$^{-/-}$ and Gaa$^{+/+}$ mice at the age of four, nine and fourteen months (four-month-old, n=3 for both Gaa$^{-/-}$ and Gaa$^{+/+}$; nine-month-old, n=2 for both Gaa$^{-/-}$ and Gaa$^{+/+}$; fourteen-month-old, n=9 for Gaa$^{+/+}$ and n=3 for Gaa$^{-/-}$). **(E)** Kaplan-Meier curve showing the comparison of survival rate between Gaa$^{-/-}$ and Gaa$^{+/+}$ mice throughout an observational period of 14 months (n=18 per group). **(F)** Grip-test measurements in Gaa$^{-/-}$ and Gaa$^{+/+}$ mice at 4, 9, and 14 months of age (4 months, n=10 for Gaa$^{-/-}$ and n=5 for Gaa$^{+/+}$; 9 months, n=9 for Gaa$^{-/-}$ and n=5 for Gaa$^{+/+}$; 14 months, n=9 for Gaa$^{+/+}$ and n=3 for Gaa). Statistical analysis: **(A-D)** Two-way ANOVA with Tukey's post hoc (phenotype, time); ns, not significant; **, p<0.01; ****, p<0.0001. **(E)** Log-rank Mantel-Cox test; ****, p<0.0001. **(F)** One-way ANOVA with Tukey's post hoc. ****, p<0.0001. In all graphs error bars represent the standard deviation of the mean.

Supplemental figure 3

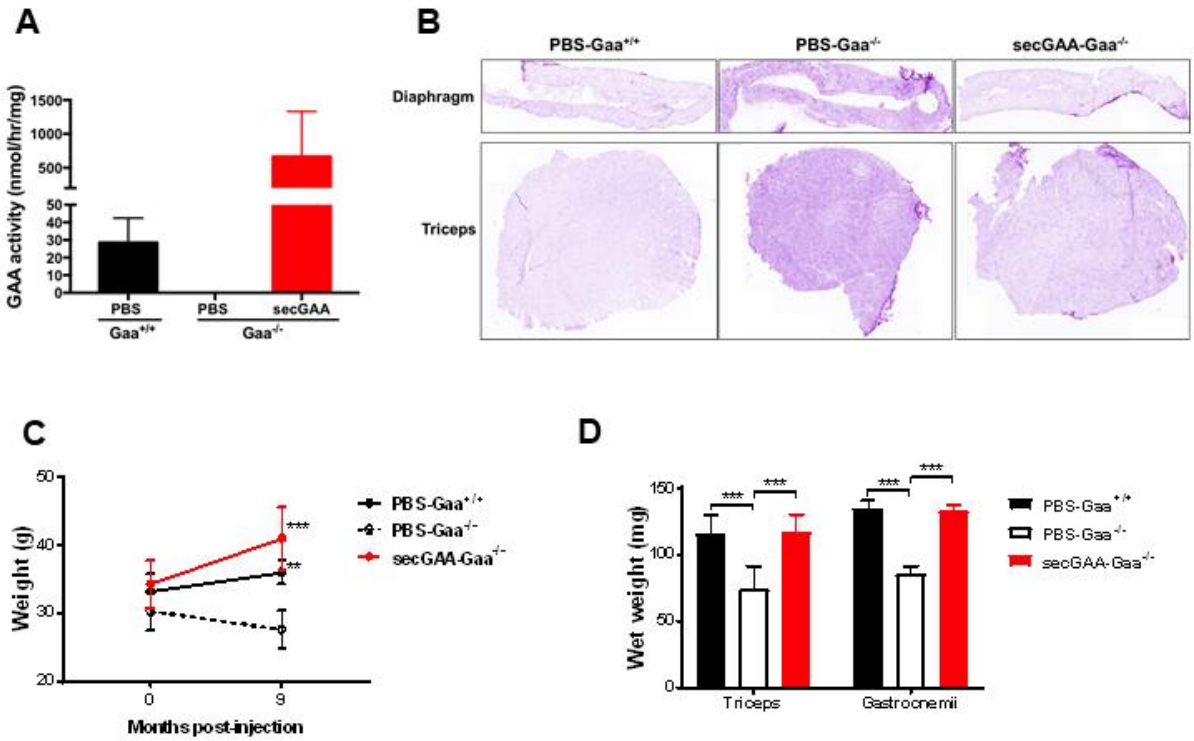

Figure S3. Liver expression of secretable GAA rescues the disease phenotype in 18-month-old Gaa$^{-/-}$ mice. (A-D) Nine-month-old mice were injected with an AAV8-secGAA (secGAA-Gaa$^{-/-}$) vector at a dose of $2x10^{12}$ vg/kg. Gaa$^{+/+}$ (PBS-Gaa$^{+/+}$) and Gaa$^{-/-}$ (PBS-Gaa$^{-/-}$) mice injected with PBS served as controls in the study. Animals were followed for nine months after treatment (n=3/4 per cohort). **(A)** GAA enzymatic activity in liver. **(B)** Representative images of periodic acid-Schiff (PAS) staining of diaphragm and triceps. **(C)** Mean mouse whole body weight zero and nine months post treatment. **(D)** *Triceps* and *gastrocnemius* muscle weight nine months post treatment. Statistical analysis: **(A)** One-way ANOVA with Tukey's post hoc; **(C-D)** Two-way ANOVA with Tukey's post hoc **(C)** (treatment, time); **(D)** (treatment, tissue). **, $p<0.01$; ***, $p<0.001$. In all graphs error bars represent the standard deviation of the mean.

Supplemental figure 4

A

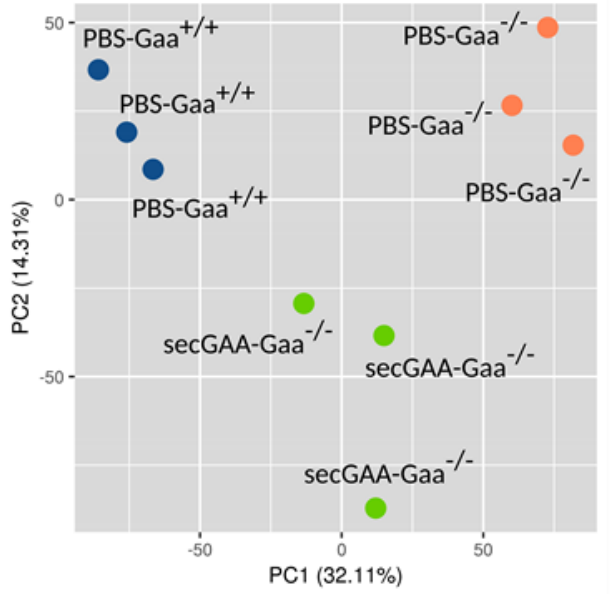

B

Differential Expression Analysis

Condition A	Condition B	DEG
PBS-Gaa$^{-/-}$	PBS-Gaa$^{+/+}$	2802
secGAA-Gaa$^{-/-}$	PBS-Gaa$^{-/-}$	434
secGAA-Gaa$^{-/-}$	PBS-Gaa$^{+/+}$	371

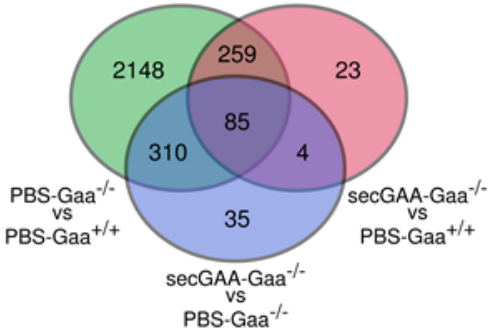

C

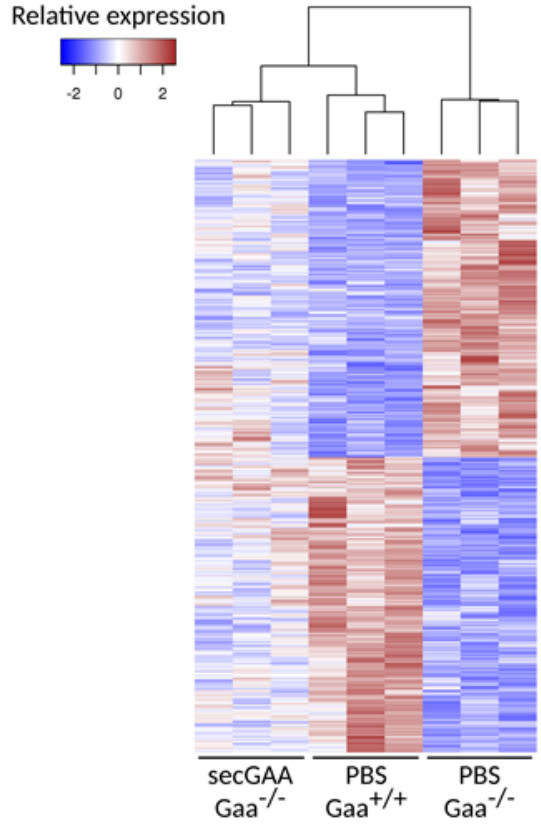

Figure S4. Normalization of transcriptomic profile in muscle following AAV8-secGAA gene transfer. (A-C) Nine-month-old mice were injected with an AAV8-secGAA (secGAA-Gaa$^{-/-}$) vector at a dose of 2x10^{12} vg/kg. Gaa$^{+/+}$ (PBS-Gaa$^{+/+}$) and Gaa$^{-/-}$ (PBS-Gaa$^{-/-}$) mice injected with PBS served as controls in the study. Animals were followed for nine months after treatment (n=3/4 per cohort). Gene expression profiles of quadriceps muscle tissue from PBS-Gaa$^{-/-}$, PBS-Gaa$^{+/+}$ and secGAA-Gaa$^{-/-}$ mice were characterized by RNA sequencing. **(A)** Principal Component Analysis was applied to compare the expression profiles of three replicate samples of each condition. Profiles were based on 13,116 genes that were expressed with at least 1 count per million in at least three samples from any condition. **(B)** Expression data from 13,116 selected genes was used to test for differential expression in pairwise comparisons between the three conditions. The number of genes detected as differentially expressed with Benjamini-Hochberg adjusted p value lower than 0.05, in each of the contrasts, is presented in the upper table. The distribution of specific and shared differentially expressed genes across the three comparisons is presented in the lower Venn diagram. **(C)** The heatmap presents normalized expression values for 2458 genes that were detected as differentially expressed in comparison PBS-Gaa$^{-/-}$ vs. PBS-Gaa$^{+/+}$. Expression counts have been scaled for each gene. Blue and red colors represent average relative expression. The dendrogram on top represents Euclidean distance between the expression profiles of each sample.

Supplemental figure 5

A

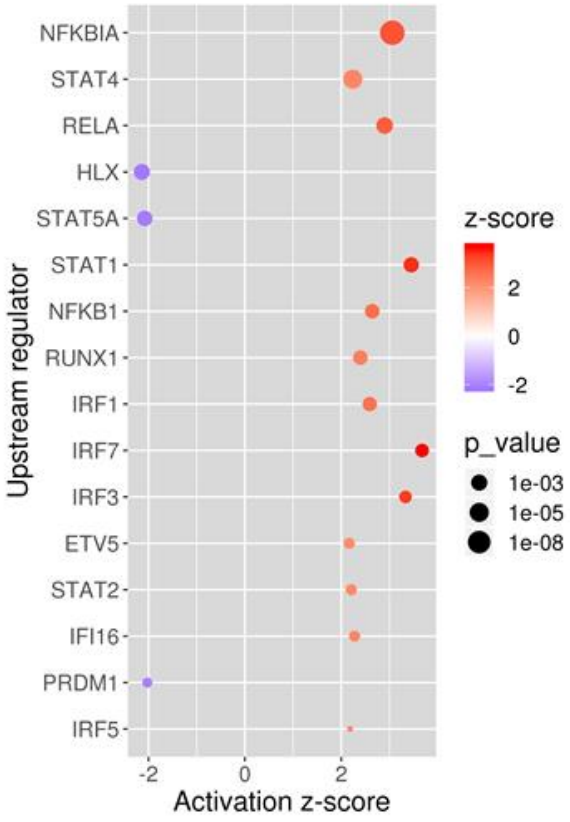

B

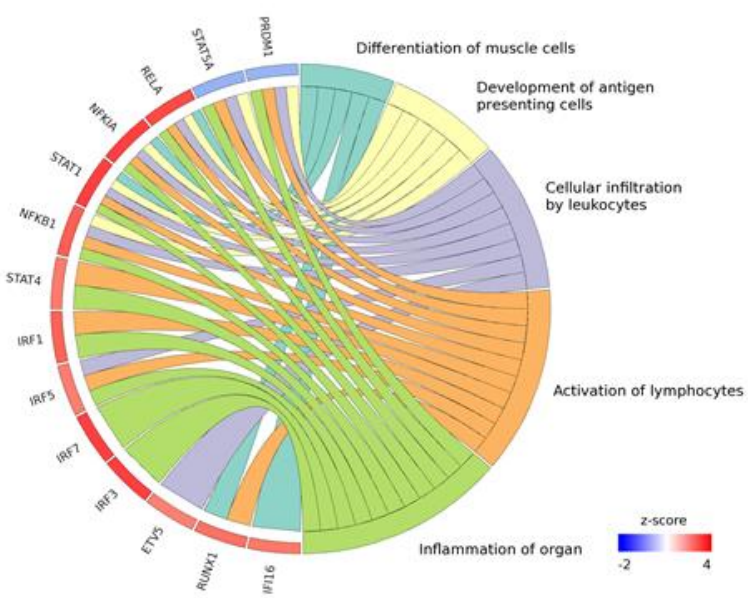

Figure S5. Inflammation related gene expression enrichment analysis. (A) Significant associations to 257 upstream transcriptional regulators were found for the set of 2802 genes detected as differentially expressed in contrast PBS-Gaa$^{-/-}$ versus PBS-Gaa$^{+/+}$, after IPA enrichment analyses. The dot plot represents enrichment p values and activation z-scores for a subset of 16 regulators involved in immunological processes. Red and purple colors indicate a higher activation state in PBS-Gaa$^{-/-}$ or PBS-Gaa$^{+/+}$ mice, respectively. **(B)** The circular plot represents 14 regulators involved in immunological processes, and a selection of their connected functions, retrieved from IPA's knowledgebase with the "grow" function. Circular crown sectors, representing transcriptional regulators, are colored according to activation z-score. Red and blue colors indicate a higher activation state in PBS-Gaa$^{-/-}$ or PBS-Gaa$^{+/+}$ mice, respectively.

Supplemental figure 6

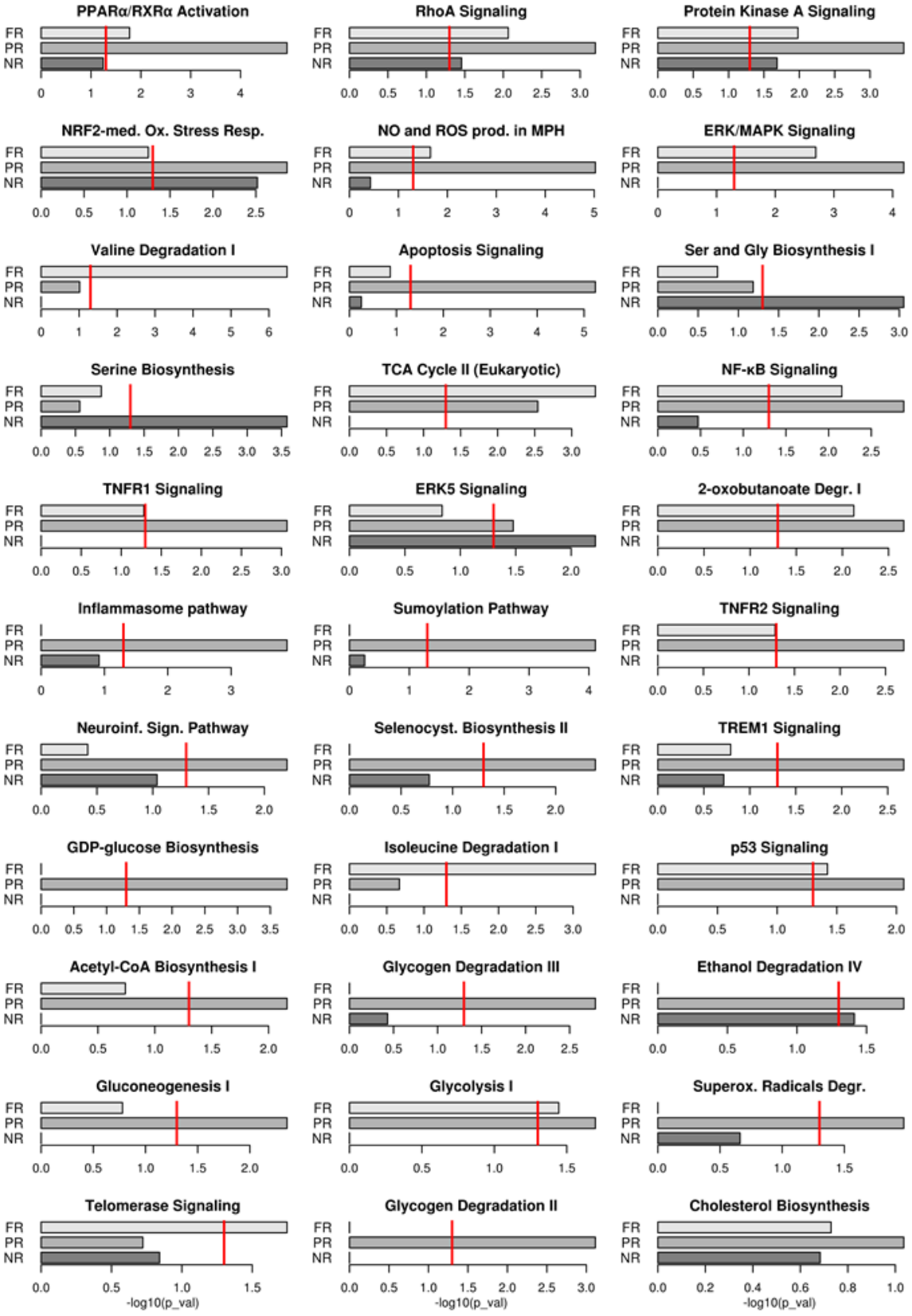

Figure S6. Ingenuity Pathway Analysis (IPA) enrichment analysis of metacluster gene lists. Significant associations to 41 Canonical Pathways were found for the three metacluster gene lists (full rescue (FR), partial rescue (PR), no rescue (NR)) after IPA enrichment analyses. Bar plots represent Fisher's test p values for 33 of the pathways of the three metaclusters. Red lines indicate the significance threshold ($p < 0.05$). Results for a complementary set of nine selected pathways are presented in Figure 6B.

Supplemental figure 7

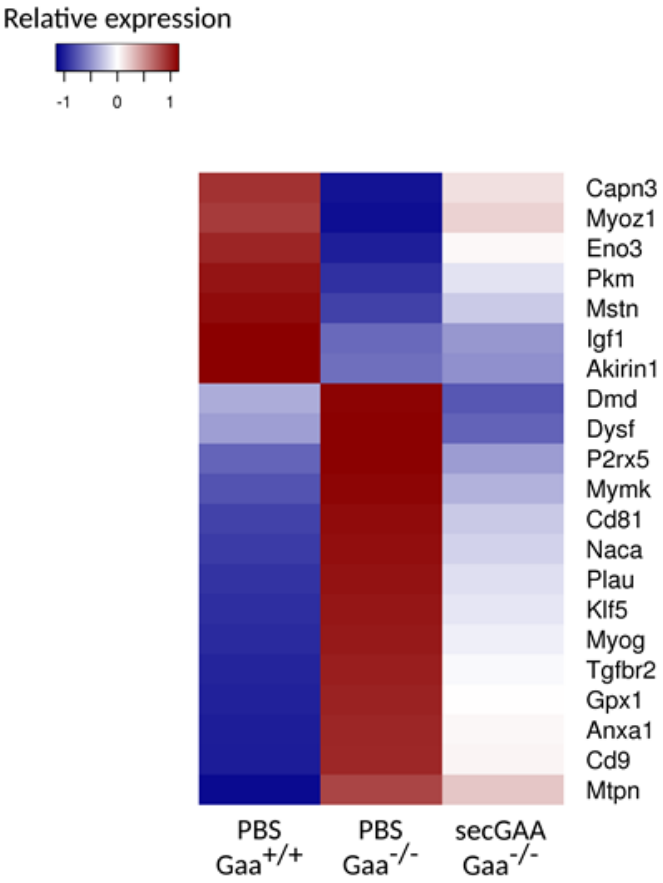

Figure S7. Expression profile of genes related to muscle regeneration. Nine-month-old mice were injected with an AAV8-secGAA (secGAA-Gaa$^{-/-}$) vector at a dose of 2x10^{12} vg/kg. Gaa$^{+/+}$ (PBS-Gaa$^{+/+}$) and Gaa$^{-/-}$ (PBS-Gaa$^{-/-}$) mice injected with PBS served as controls in the study. Animals were followed for nine months after treatment (n=3/4 per cohort). A list of 44 mouse genes related to skeletal muscle tissue regeneration (GO:0043403) was retrieved from BioMart and expanded by the addition of MYOG. The heatmap presents RNASeq-based, normalized expression values for 21 genes involved in muscle regeneration that had been detected as differentially expressed in PBS-Gaa$^{-/-}$ vs. PBS-Gaa$^{+/+}$. Expression counts have been averaged for each condition, and scaled for each gene. Blue and red colors represent relative expression values below and above average, respectively.

Supplemental figure 8

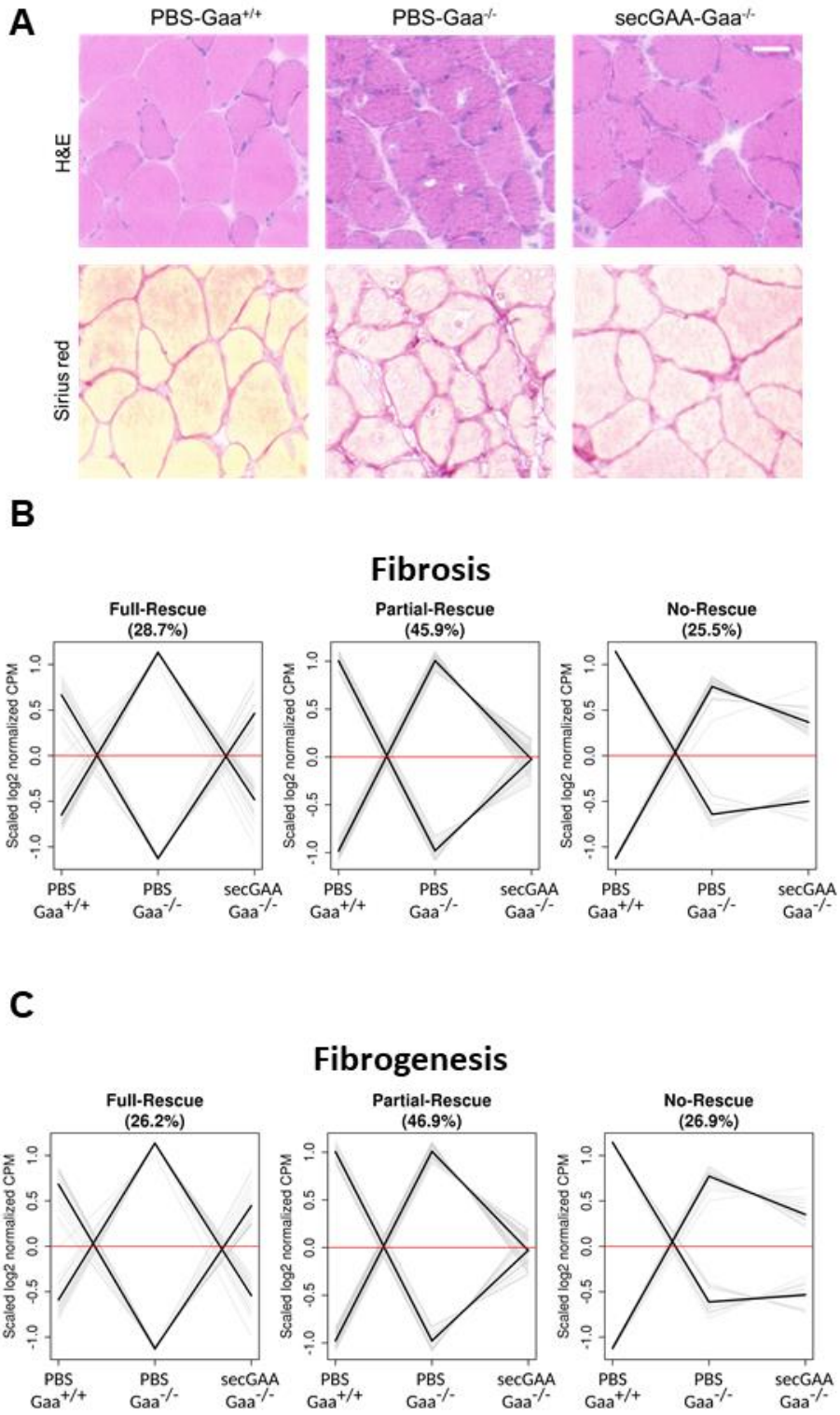

Figure S8. AAV mediated hepatic expression of secGAA partially normalizes fibrotic changes in the muscle. **(A-C)** Nine-month-old mice were injected with an AAV8-secGAA (secGAA-Gaa-/-) vector at a dose of $2x10^{12}$ vg/kg. Gaa+/+ (PBS-Gaa+/+) and Gaa-/- (PBS-Gaa-/-) mice injected with PBS served as controls in the study. Animals were followed for nine months after treatment (n=3/4 per cohort). **(A)** Representative images of hematoxylin and eosin (H&E) and Sirius Red staining of triceps muscle of mice. Scale bar represents 10µm. **(B)** Distribution of 157 genes associated to functional term "Fibrosis" in gene metaclusters fully rescued (FR), partially rescued (PR) and not rescued (NR), as defined in Figure 6. Fibrosis-associated genes had been identified as significantly enriched in Ingenuity Pathway Analysis (IPA) on the set of 2802 genes detected as differentially expressed in contrast PBS-Gaa-/- versus PBS-Gaa+/+ (Benjamini-Hochberg adjusted p_value = $1x10^{-13}$). Normalized expression counts, averaged for each condition and scaled for each gene, are represented on the Y-axis. Gray lines represent the expression profile of individual Fibrosis-associated genes. Black lines represent average expression profiles for Fibrosis-associated genes included in each of the original clusters. Percentages represent the fraction of Fibrosis-associated genes included in each metacluster. **(C)** Distribution of 145 genes associated to functional term "Fibrogenesis" in the same metaclusters. Fibrogenesis-associated genes had been identified as significantly enriched in IPA analyses on the set.